J|A|C|S
ARTICLES
Published on Web 04/06/2007

Evidence for Sevenfold Coordination in the First Solvation Shell of Hg(II) Aqua Ion

Giovanni Chillemi,[†] Giordano Mancini,[†,‡] Nico Sanna,[†] Vincenzo Barone,*[,§] Stefano Della Longa,[||] Maurizio Benfatto,[⊥] Nicolae V. Pavel,[‡] and Paola D'Angelo*[,‡]

Contribution from the CASPUR, Consortium for Supercomputing. Applications,Via dei Tizii 6b, 00185 Rome, Italy, Department of Chemistry, University of Rome "La Sapienza", P.le Aldo Moro 5, 00185 Rome, Italy, Department of Chemistry, University of Naples Federico II, Via Cintia, 80126 Naples, Italy, Department of Experimental Medicine, University of L'Aquila, 67100 L'Aquila, Italy, and INFN, Frascati National Laboratories, 00044 Frascati, Italy

Received October 2, 2006; E-mail: baronev@unina.it; p.dangelo@caspur.it

Abstract: A quite unexpected sevenfold coordination of the hydrated Hg(II) complex in aqueous solution is revealed by an extensive study combining X-ray absorption spectroscopy (XAS) and quantum mechanics/molecular dynamics (QM/MD) calculations. As a matter of fact, the generally accepted octahedral solvation of Hg(II) ion cannot be reconciled with XAS results. Next, refined QM computations point out the remarkable stability of a heptacoordinated structure with C_2 symmetry, and long-time MD simulations by new interaction potentials including many-body effects reveal that the hydrated complex has a quite flexible structure, corresponding for most of the time to heptacoordinated species. This picture is fully consistent with X-ray absorption near-edge structure experimental data which unambiguously show the preference for a sevenfold instead of a sixfold coordination.

Introduction

Mercury is a toxic and an environmentally hazardous element able to replace biological Zn(II) in enzymes, proteins, and nucleic acids, altering the normal activity of these species.[1] Once released to the environment by a variety of sources (e.g., waste combustors or coal-fired power plants), metallic mercury is oxidized to Hg(II) by water and ozone, and when it falls on the ground of acidic soil (around pH = 4), it transforms to the neurotoxin methyl mercury that causes severe neurological damages (e.g., Minamata disease).[2,3] Despite the calamitous effects on human health arising from mercury pollution of streams, lakes, and oceans,[4] the solution structure of aqua Hg(II) ion is still poorly defined due to the lack of experimental techniques able to provide reliable information about the coordination structure of this ion.[5] Hg(II) is normally described as being hexacoordinated by water,[5,6] but due to the occurrence of hydrolysis and of different coordination geometries that mercury adopts in complexes, a conclusive description of the structural properties of this ion is still lacking.[5] Moreover, like Zn(II) and Cd(II), the d^{10} Hg(II) ion has no electronic spectroscopic handle, and the few attempts made to study its hydration structure by X-ray diffraction are in support of retention of the same octahedral structure as present in the solid-state X-ray structure of $Hg(ClO_4)_2 \cdot 6H_2O$.[6] However, the radial distribution function obtained from X-ray diffraction of Hg(II) in aqueous solution showed a broad peak corresponding to an unexpectedly large variation in the Hg−O bond lengths.[7] The wide bond distance distribution has been explained by a pseudo Jahn−Teller effect in the hexahydrated mercury(II) complexes leading to four equatorial Hg−O bonds about 0.05 Å shorter than the axial ones.[7] In addition, the residence time of water molecules in the first hydration shell of Hg(II) is quite short (of the order of nanoseconds)[8] as compared with divalent first row transition ions which form octahedral hydration complexes in aqueous solution.[5]

We have undertaken a combined experimental and theoretical investigation to unveil the detailed structure and dynamics of the hydrated Hg(II) ion complex in aqueous solution. We used a combined extended X-ray absorption fine structure (EXAFS) and X-ray absorption near-edge structure (XANES) analysis to explore the Hg(II) hydration structure. Quantum mechanical *ab initio* calculations support the experimentally determined structural results, and molecular dynamics simulations reveal the dynamic behavior of the system.

[†] CASPUR.
[‡] Department of Chemistry, University of Rome "La Sapienza".
[§] Department of Chemistry, University of Naples Federico II.
[||] Department of Experimental Medicine, University of L'Aquila.
[⊥] Frascati National Laboratories.

(1) Jennette, K. W. *Environ. Health Perspect.* **1981**, *40*, 233−252.
(2) Benoit, J. M.; Fitzgerald, W. F.; Damman, A. W. H. *Mercury Pollution: Integration and Synthesis*; Watras, C. J., Huckabee, J. W., Eds.; Lewis: Boca Raton, FL, 1994; pp 187−202.
(3) Goyer, R. A. *Toxicological Effects of Methylmercury*; National Academy Press: Washington, DC, 2000.
(4) Seller, P.; Kelly, C. A.; Rudd, J. W. M.; MacHutchon, A. R. *Nature* **1996**, *380*, 694−697.
(5) Richens, D. T. *The Chemistry of Aqua Ions*; Wiley: Chichester, 1997.
(6) Johansson, G.; Sandström, M. *Acta Chem. Scand., Ser. A* **1978**, *32*, 109−113.
(7) Sandström, M.; Persson, I.; Ahrland, S. *Acta Chem. Scand., Ser. A* **1978**, *32*, 627−41.
(8) Eigen, M. *Pure Appl. Chem.* **1963**, *6*, 97−115.

10.1021/ja066943z CCC: $37.00

Materials and Methods

X-ray Absorption Measurements. A 0.1 M Hg(II) water solution was prepared by dissolving the appropriate amount of $Hg(ClO_4)_2$ in freshly distilled water and adding $HClO_4$ in order to prevent hydrolysis. Hg L_{III} XAS spectra were obtained at the X-ray absorption spectrometer BM29[9] of the European Synchrotron Radiation Facility (ESRF). Spectra were recorded in transmission mode using a Si(311) double-crystal monochromator detuned to 50%. Data points were collected for 1 s each, and three spectra were recorded and averaged. The solution was kept in a cell with Kapton film windows and Teflon spacers of 4 mm.

XANES Data Analysis. The raw experimental data (see Supporting Information Figure S1) were deconvolved of the whole tabulated Hg L_{III} core hole width ($\Gamma = 5.50$ eV).[10,11] This treatment largely facilitates the detection of spectral features and the comparison with theoretical calculations. The XANES data analysis was carried out with the MXAN code.[12] The X-ray absorption cross section was calculated in the framework of the full multiple-scattering scheme within the muffin-tin approximation for the shape of the potential. The real part of the exchange term was calculated using the Hedin−Lundqvist energy-dependent potential, while the inelastic losses did not include the core-hole lifetime broadening as it was previously eliminated from the experimental spectrum. A least-square fit of the experimental data in the space of the structural parameters was achieved using the MINUIT routine of the CERN library,[13] which minimizes the R_{sq} function defined as

$$R_{sq} = \frac{n}{m\epsilon^2}\sum_{i=1}^{m}[(y_i^{theor} - y_i^{expmtl})\epsilon_i^{-1}]^2 \quad (1)$$

where n is the number of the independent structural parameters, m is the number of experimental points (88 for all the reported analyses), y_i^{theor} and y_i^{expmtl} are the theoretical and experimental values of the absorption cross section, and ϵ_i was constant and equal to 0.5% of the experimental jump. The MIGRAD subroutine of the MINUIT package calculates the reported statistical errors. The resolution broadening was taken into account using a Gaussian function.

Quantum Mechanical Details. All the quantum mechanical computations have been carried out with the Gaussian 03 package.[14] In view of previous experience,[15,16] we have selected the pseudo-relativistic LANL2[17] effective potential for mercury and optimized a corresponding valence basis set (describing 5d, 6s, and, possibly, 6p orbitals) including multiple *f* and *g* polarization functions (see Table 1), whereas H_2O has been described by the cc-pVTZ basis set, augmented by diffuse s and p functions on the oxygen atoms taken from the aug-cc-pVTZ set.[18]

Test computations performed on the Hg(II)−H_2O system have shown that at this level the basis set superposition error (BSSE) is very low (see Table 2). Furthermore, the very reliable CCSD(T) (Coupled Cluster Singles and Doubles with noniterative account of Triple excitations) approach[19] and the less CPU demanding second order Moeller−Plesset (MP2) method[20] provide essentially equivalent results, while sizable differences are obtained from Hartree−Fock (HF) calculations (see Table 2). All following computations have thus been performed at the MP2 level.

Table 1. Optimized Valence Basis Set Used for Mercury with the LANL2 Effective Core Potential

shell	exponent	coefficent (*s*)	coefficent (*p*)
S	$3.669\,645\,6 \times 10^{+1}$	-1.000×10^{-4}	
	$5.550\,243\,6 \times 10^{0}$	-4.500×10^{-4}	
	$2.964\,286\,7 \times 10^{0}$	-3.047×10^{-2}	
	$1.583\,829\,5 \times 10^{0}$	1.717×10^{-1}	
	$8.464\,231\,7 \times 10^{-1}$	-4.839×10^{-1}	
SP	$8.464\,231\,7 \times 10^{-1}$	1.000×10^{0}	1.000×10^{0}
SP	$4.523\,856\,7 \times 10^{-1}$	1.000×10^{0}	1.000×10^{0}
SP	$2.417\,952\,1 \times 10^{-1}$	1.000×10^{0}	1.000×10^{0}
SP	$1.292\,387\,9 \times 10^{-1}$	1.000×10^{0}	1.000×10^{0}
SP	$6.907\,803\,0 \times 10^{-2}$	1.000×10^{0}	1.000×10^{0}
D	$3.669\,645\,6 \times 10^{+1}$	-9.700×10^{-4}	
	$5.550\,243\,6 \times 10^{0}$	-4.590×10^{-3}	
	$2.964\,286\,7 \times 10^{0}$	2.690×10^{-3}	
	$2.417\,952\,1 \times 10^{-1}$	9.832×10^{-2}	
	$1.292\,387\,9 \times 10^{-1}$	2.794×10^{-2}	
D	$1.583\,829\,5 \times 10^{0}$	1.000×10^{0}	
D	$8.464\,231\,7 \times 10^{-1}$	1.000×10^{0}	
D	$4.523\,856\,7 \times 10^{-1}$	1.000×10^{0}	
F	$1.583\,829\,5 \times 10^{0}$	1.000×10^{0}	
F	$4.523\,856\,7 \times 10^{-1}$	1.000×10^{0}	
G	$1.583\,829\,5 \times 10^{0}$	1.000×10^{0}	

The potential energy surface (PES) of the Hg(II)−H_2O system has been characterized by means of 1833 grid points with a tilt angle ϕ equal to 0° (ion−oxygen distances ranging from 1.2 to 4 Å and steps of 0.02 Å; ion−oxygen−hydrogen θ angles ranging from 7.745° to 127.745° and steps of 10°), and 572 grid points with a tilt angle different from 0° (ϕ equal to 30°, 45°, 60°, 90°, and 135°; ion−oxygen distances ranging from 1.7 to 2.7 Å and steps of 0.1 Å; ion−oxygen−hydrogen θ angles ranging from 7.745° to 127.745° and step of 10°). The initial 2405 grid points were reduced to 2163 by imposing a threshold of 4000 kJ mol^{-1} for the interaction energy, thus not including the most repulsive conformations in the PES.

After MP2 computations in vacuum, bulk solvent effects have been taken into account by means of the latest implementation of the so-called conductor-like polarizable continuum model (CPCM).[21−23] The effective potential governing Hg(II)−H_2O interactions including non-additive effects by other solvent molecules can be expressed as[24]

$$U_{HgW} = \langle\psi|^{(0)}|\psi\rangle_{HgW} - \langle\psi|\hat{\mathcal{H}}^{(0)}|\psi\rangle_{Hg} - \langle\psi|\hat{\mathcal{H}}^{(0)}|\psi\rangle_{W} \quad (2)$$

where the wave function ψ is perturbed by the solvent effect according to the CPCM, and the Hamiltonian operators $\hat{\mathcal{H}}^{(0)}$ refer to the Hg(II)−H_2O, bare Hg(II) ion, and bare water molecule in a vacuum. At variance with previous studies[25,26] the energy has been computed at the MP2 level using the HF wave function polarized by the solvent reaction field. The optimization of the CPCM Hg(II) cavity radius has been performed along the line of the previously described procedure,[15] giving rise to a cavity radius of 1.14 Å, while radii of 1.68 and 1.44 Å have been used with an α scaling factor of 0.965 for the oxygen and hydrogen atoms, respectively. Each sphere forming the solute cavity has been subdivided into finite elements (*tesserae*) with a constant average area of 0.05 $Å^2$, without any charge compensation.[23]

(9) Filipponi, A.; Borowski, M.; Bowron, D. T.; Ansell, S.; Di Cicco, A.; De Panfilis, S.; Itiè, J.-P. *Rev. Sci. Instrum.* **2000**, *71*, 2422−2432.
(10) Krause, M. O.; Oliver, J. H. *J. Phys. Chem. Ref. Data* **1979**, *8*, 329−338.
(11) Filipponi, A. *J. Phys. B: At. Mol. Opt. Phys.* **2000**, *33*, 2835−2846.
(12) Benfatto, M.; Della Longa, S.; Natoli, C. R. *J. Synchrotron Radiat.* **2003**, *10*, 51−57.
(13) www.cern.ch/minuit.
(14) Frisch, M. J., et. al. *Gaussian 03*, revision C.02; Gaussian, Inc.: Wallingford, Connecticut, 2004.
(15) Chillemi, G.; D'Angelo, P.; Pavel, N. V.; Sanna, N.; Barone, V. *J. Am. Chem. Soc.* **2002**, *124*, 1968−1976.
(16) Chillemi, G.; Barone, V.; D'Angelo, P.; Mancini, G.; Persson, I.; Sanna, N. *J. Phys. Chem. B* **2005**, *109*, 9186−9193.
(17) Hay, P. J.; Wadt, W. R. *J. Chem. Phys.* **1985**, *82*, 299−310.
(18) Wilson, A.; van Mourik, T.; Dunning, T. H., Jr. *THEOCHEM* **1996**, *388*, 339−349.
(19) Pople, J. A.; Head-Gordon, M.; Raghavachari, K. *J. Chem. Phys.* **1987**, *87*, 5968−5975.
(20) Saebo, S.; Almlof, J. *Chem. Phys. Lett.* **1989**, *154*, 83−89.
(21) Tomasi, J.; Mennucci, B.; Cammi, R. *Chem. Rev.* **2005**, *105*, 2999−3093.
(22) Cossi, M.; Rega, N.; Scalmani, G.; Barone, V. *J. Chem. Phys.* **2002**, *117*, 43−54.
(23) Cossi, M.; Rega, N.; Scalmani, G.; Barone, V. *J. Comput. Chem.* **2003**, *24*, 669−681.
(24) Floris, F.; Persico, M.; Tani, A.; Tomasi, J. *Chem. Phys. Lett.* **1992**, *199*, 518−524.
(25) Rega, N.; Cossi, M.; Barone, V. *J. Am. Chem. Soc.* **1997**, *119*, 12962−12967.
(26) Barone, V.; Adamo, C. *Chem. Phys. Lett.* **1994**, *224*, 432−438.

Table 2. Hg(II)−Water Interaction Energy Values for Different *ab Initio* Methods and Hg(II)−O Distances (R_{Hg-O})

R_{Hg-O} (Å)	HF[a] (kJ/mol)	HF[a,b] (kJ/mol)	MP2[a] (kJ/mol)	MP2[a,b] (kJ/mol)	CCSD(T)[a] (kJ/mol)	CCSD(T)[a,b] (kJ/mol)	U_{HgW}[c] (kJ/mol)
1.8	−183.5	−183.1	−250.9	−242.4	−235.3	−227.5	−123.2
2.0	−283.1	−282.8	−335.5	−329.7	−325.2	−319.9	−222.8
2.2	−293.6	−293.3	−335.4	−331.5	−328.9	−325.3	−227.5
2.5	−253.1	−252.9	−283.1	−280.9	−282.7	−278.6	−183.8
2.6	−235.6	−235.5	−262.3	−260.5	−260.8	−259.1	−167.6
3.0	−171.6	−171.4	−186.7	−185.8	−187.9	−187.0	−117.0
3.5	−116.4	−116.3	−121.8	−121.4	−123.9	−123.5	−84.6
4.0	−83.4	−83.4	−84.0	−83.7	−85.8	−85.6	−70.0

[a] In a vacuum. [b]Corrected for BSSE. [c]See eq 2.

Table 3. Estimated Hg(II)−H_2O Interaction Parameters and Relative Standard Deviations for the PCM/MP2 Effective Two Body Potential[a]

	effective two body		pure pair additive	
	parameters	std dev	parameters	std dev
A_o	1.2712	4.50×10^{-2}	2.707×10^{-1}	8.39×10^{-2}
B_o	-1.181×10^{-1}	5.31×10^{-3}	-8.640×10^{-2}	1.09×10^{-3}
C_o	8.443×10^{-4}	7.40×10^{-5}	9.190×10^{-5}	1.32×10^{-5}
D_o	-1.178×10^{-8}	3.58×10^{-9}	-3.050×10^{-8}	5.63×10^{-9}
E_o	$2.130 \times 10^{+6}$	$6.86 \times 10^{+4}$	$8.085 \times 10^{+5}$	$3.96 \times 10^{+4}$
F_o	$3.952 \times 10^{+1}$	3.02×10^{-1}	$3.455 \times 10^{+1}$	3.35×10^{-1}
A_h	4.408×10^{-2}	2.07×10^{-3}	-7.680×10^{-2}	3.29×10^{-3}
B_h	-5.700×10^{-4}	4.10×10^{-5}	2.150×10^{-4}	6.10×10^{-6}
B_h	3.372×10^{-6}	2.29×10^{-7}	-9.700×10^{-6}	3.15×10^{-7}
B_h	-2.348×10^{-11}	1.88×10^{-12}	5.410×10^{-11}	2.25×10^{-12}

[a] For comparison, the same data are reported for the pure pair additive potential obtained by MP2 in vacuo calculations.

Molecular Dynamics Details. The MD simulations have been carried out using the GROMACS package version 3.2,[27] modified in order to include our Hg(II)−H_2O effective two-body potential functions, by means of the following expression

$$V(r) = \frac{q_i q_o}{r_{io}} + \frac{A_o}{r_{io}^4} + \frac{B_o}{r_{io}^6} + \frac{C_o}{r_{io}^8} + \frac{D_o}{r_{io}^{12}} + E_o e^{-F_o r_{io}} + \sum_{ih=ih1,\, ih2} \frac{q_i q_h}{r_{ih}} + \frac{A_h}{r_{ih}^4} + \frac{B_h}{r_{ih}^6} + \frac{C_h}{r_{ih}^8} + \frac{D_h}{r_{ih}^{12}} \quad (3)$$

where r_{io}, r_{ih1}, and r_{ih2} are the ion−water distances; q_i, q_o, and q_h are the electrostatic charges of mercury, oxygen, and hydrogen atoms, respectively (2, −0.8476 and 0.4238 au); and the A_o,...., F_o, A_h,...,D_h parameters are reported in Table 3, for both the effective two body potential that accounts for many-body terms by means of PCM calculations and, for comparison, a pure pair additive potential, obtained by the in vacuum MP2 calculations.

A system including one Hg(II) ion and 819 SPC/E water molecules[28] has been simulated enforcing periodic boundary conditions in the NVT ensemble. A cutoff of 9 Å has been used for the nonbonded interactions, using the particle-mesh Ewald method to treat the long-range electrostatic interactions.[29,30] A homogeneous background charge was applied to compensate for the ionic charge.[31] The temperature was kept fixed at 300 K by weak coupling to an external temperature bath using Berendsen's method[32] with a coupling constant of 0.1 ps. The simulation has been carried out for 65 ns, with a time step of 1 fs. The first 5 ns have been utilized to equilibrate the system and discarded in all the analyses. In order to test the stability of the heptacoordinated first hydration species, after 15 ns of unperturbed MD simulation, the final coordinates have been used to carry out six additional simulations of 2500 ps each, where the starting velocities have been randomly generated. After the starting perturbation, the heptacoordinated structure was restored in all of the simulations and it was the only observed first hydration shell species. A last MD simulation has been carried out with the Hg(II)−water pure pair additive potential, obtained by MP2 in vacuum calculations (eq 3 and Table 3) for 25 ns of simulation time. The trajectories of the last 20 ns have been saved every 25 ps for analyses.

The residence time τ of water molecules in the first coordination shell of Hg(II) has been estimated following the method of Impey and coauthors.[33] According to this method it is possible to define for each water molecule a binary survival probability function $P_j(t, t_n, t^*)$ that takes the value 1 if the water molecule j lies within the referred hydration shell at both time steps t_n and $t + t_n$ and does not leave the coordination shell for any continuous period longer than t^*. Otherwise, it takes the value 0. From P_j it is possible to define an average quantity $n_{ion}(t)$ given by the expression

$$n_{ion}(t) = \frac{1}{N_t} \sum_{n=1}^{N_t} \sum_j P_j(t_n, t, t^*) \quad (4)$$

where N_t represents the total number of steps. At long times, $n_{ion}(t)$ decays in an exponential fashion, with a characteristic correlation time τ which defines the residence time of the water molecule in the shell. We have chosen a t^* value equal to the time interval between saved configurations (25 fs). A water molecule has been considered in the first hydration shell if the Hg(II)−oxygen distance was shorter than 3.8 Å.

Results and Discussion

The EXAFS data analysis of the Hg L_{III}-edge spectrum has been performed with the GNXAS code,[34] using previously developed and widely applied methods.[35] Three fits were carried out using a single coordination shell with fixed coordination numbers of 6, 7, and 8. Very similar agreement between the experimental and theoretical signals has been obtained in the three cases; the Hg−O distance was always 2.32(2) Å with σ^2 values of 0.025, 0.027, and 0.033 Å^2 and third cumulant C_3 values of 0.0065, 0.0074, and 0.0096 Å^3, for the hexa-, hepta- and octacoordinated models, respectively. The results of the fitting procedure carried out using an octahedral model are

(27) Berendsen, H. J. C.; van der Spoel, D.; van Drunen, R. *Comput. Phys. Commun.* **1995**, *95*, 43−56.
(28) Berendsen, H. J. C.; Grigera, J. R.; Straatsma, T. P. J. *Phys. Chem.* **1987**, *91*, 6269−6271.
(29) Darden, T.; York, D.; Pedersen, L. J. *J. Chem. Phys.* **1993**, *98*, 10089−10092.
(30) Essmann, U.; Perera, L.; Berkowitz, M. L.; Darden, T.; Lee, H.; Pedersen, L. G. J. *J. Chem. Phys.* **1995**, *103*, 8577−8592.
(31) Hummer, G.; Pratt, L. R.; Garcia, A. E. *J. Phys. Chem. A* **1998**, *102*, 7885−7895.
(32) Berendsen, H. J. C.; Postma, J. P. M.; van Gusteren, W. F.; Di Nola, A.; Haak, J. R. *J. Comput. Phys.* **1984**, *81*, 3684−3690.
(33) Impey, R. W.; Madden, P. A.; McDonald, I. R. *J. Phys. Chem.* **1983**, *87*, 5071−5083.
(34) Filipponi, A.; Di Cicco, A.; Natoli, C. R. *Phys. Rev. B* **1995**, *52*, 15122−15134.
(35) D'Angelo, P.; Di Nola, A.; Filipponi, A.; Pavel, N. V.; Roccatano, D. *J. Chem. Phys.* **1994**, *100*, 985−994.

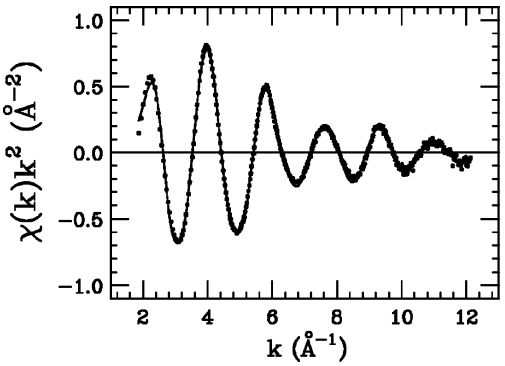

Figure 1. Experimental k^2 weighted EXAFS data of Hg(II) in water (dotted line) are compared with a the best fit signal corresponding to an octahedral model (solid line). The EXAFS data of the assumed octahedral Hg(II) complexes show an obvious damping of the amplitude at high k values.

shown in Figure 1. The coordination number of the Hg(II) hydration complex cannot be accurately determined from the EXAFS data analysis due to its large correlation with the Debye−Waller factor. However, the structural oscillations decrease very rapidly (Figure 1), giving somehow larger Debye−Waller factors than expected for an octahedral coordination complex.[36] The presence of a Hg−Hg interaction has been discarded as the Hg−Hg two body signal presents a high amplitude in the k-range between 6 and 10 Å^{-1} in contrast to the experimental data behavior.

XANES is extremely sensitive to the geometric environment of the absorbing atom as multiple-scattering effects make large contributions to this region of the X-ray absorption spectra. A quantitative analysis of the XANES which includes the rising edge and about 200 eV above it can address some of the aforementioned shortcomings of EXAFS.

To examine the compatibility of the XANES spectrum with the existence of an octahedral geometry of the solvated Hg(II) ion, we performed a minimization of the experimental data imposing T_h symmetry (see Figure 2A). In this fit, only the Hg(II)−water ligand distance was allowed to vary, resulting in a Hg−O best-fit distance of 2.29(3) Å and $R_{sq} = 15.7$ (see Table 4). A second minimization has been carried out using an equatorially constrained Jahn−Teller distorted octahedron (see Figure 2B). In this case the equatorial Hg−O distances obtained from the fit were equal to 2.24(3) Å, while the two axial distances were found at 2.41(3) Å, with an $R_{sq} = 15.2$ (see Table 4). Note that even if the agreement between the experimental and theoretical spectra is not satisfactory, the results of the fitting procedure point toward a structure with a very large difference (0.17 Å) between the equatorial and axial distances.

Finally, to assess the compatibility of the XANES with a more disordered hexacoordinated hydration complex, we performed an additional minimization of the experimental data using an unconstrained hexacoordinated cluster, where all of the six Hg−O bond distances were refined (see Figure 2C). In this case the Hg(II)−O distances are spread between 2.19 and 2.44 Å, with an average value of 2.31 Å, and R_{sq} is 9.9 (see Table 4). Thus all the hexahydrated models lead to a quite poor agreement between the experiment and the calculated spectra, especially in the low-energy region of the spectrum. In particular, the measured XANES spectrum exhibits a shoulder at the main

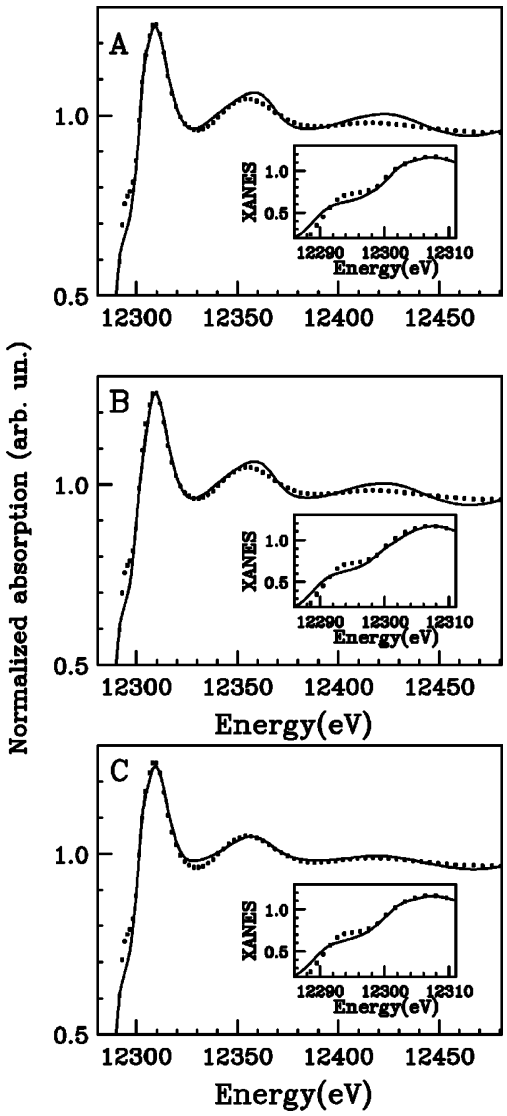

Figure 2. (A) Comparison of the Hg L_{III} deconvolved experimental XANES spectrum of the Hg(II) aqueous solution (dotted line), with the best fit theoretical spectrum (solid line) associated with an octahedral $[Hg(H_2O)_6]^{2+}$ cluster. (B) Comparison of the experimental XANES spectrum (dotted line), with the best fit theoretical spectrum (solid line) associated with a Jahn−Teller distorted octahedral cluster. (C) Comparison of the experimental XANES spectrum (dotted line), with the best fit theoretical spectrum (solid line) obtained from a disordered six-coordinated model.

transition edge that could not be reproduced (insets of Figure 2), and a poor agreement between the experiment and the calculated model is found also in the high-energy range of the spectrum (12350−12600 eV) for the regular and Jahn−Teller distorted octahedra. In the case of the unconstrained hexacoordinated model, the Hg(II)−O distances are quite spread and the structural disorder reduces the amplitude of the signal at high energy, resulting in a better agreement with the experimental data (Figure 2C). Nevertheless, the frequency is not completely correct and the shoulder at the main edge is not reproduced (see inset of Figure 2C). All together these findings suggest that, at variance with all the previously reported results,[5,7] the Hg(II) aqua ion does not adopt an octahedral coordination, and it forms a quite flexible hydration complex.

We have thus performed a comprehensive quantum mechanical study of different $[Hg(H_2O)_n]^{2+}$ ($n = 6-8$) clusters both in a vacuum and simulating bulk solvent effects by the PCM

(36) D'Angelo, P.; Barone, V.; Chillemi, G.; Sanna, N.; Meyer-Klaucke, W.; Pavel, N. V. *J. Am. Chem. Soc.* **2002**, *124*, 1958−1967.

Table 4. Structural and Background Parameters Obtained from the XANES Minimizations[a]

models	R_1	R_2	R_3	R_4	R_5	R_6	R_7	Res	E_o	R_{sq}	n
octahedron	2.29	2.29	2.29	2.29	2.29	2.29	-	0.74	12 286.5	15.7	1
JT distorted octahedron	2.24	2.24	2.24	2.24	2.41	2.41	-	0.71	12 286.5	15.2	2
flexible six-coordinated	2.19	2.22	2.26	2.29	2.44	2.44	-	0.71	12 286.6	9.9	6
C_2 seven-coordinated	2.19	2.19	2.23	2.23	2.40	2.40	2.57	0.72	12 286.5	1.6	4
flexible seven-coordinated	2.17	2.17	2.30	2.30	2.39	2.45	2.45	0.72	12 286.6	1.1	7

[a] R_i (Å) are the Hg(II)−O distances, Res (eV) is resolution broadening, E_o (eV) is the theoretical absorption edge position, R_{sq} is the fit index parameter (eq 1), and n is the number of independent structural parameters used in the fitting procedure.

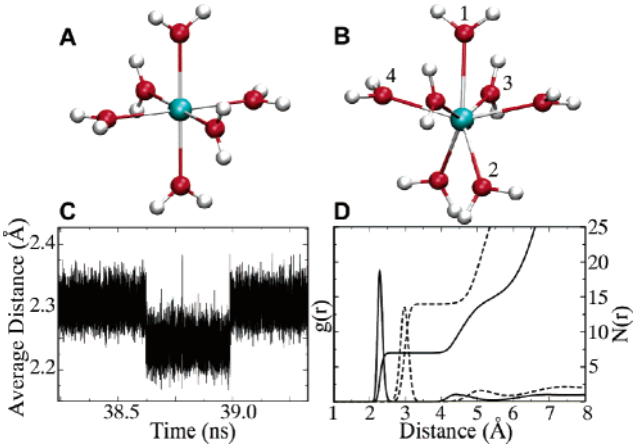

Figure 3. Perspective views of the MP2 minimum energy structures for $[Hg(H_2O)_n]^{2+}$ complexes with $n = 6$ (A) and $n = 7$ (B). (C) Average Hg−O distance for the first shell water molecules as a function of simulation time. A simulation window has been chosen around the longest lifetime of the hexacoordinated species. The lowest mean distance region corresponds to the hexacoordinated species. (D) Hg−O (full line) and Hg−H (dashed line) radial distribution functions as derived from MD simulations and corresponding hydration numbers (right scale).

Table 5. Main Geometrical Parameters and Energy Values at the MP2 Level of Computations, for the Hexa-, Hepta-, and Octacoordinated Clusters[a]

		MP2	
		vacuo	PCM
$[Hg(H_2O)_6]^{2+}$	E (au)	−499.5130	−499.8173
	R_{Hg-O} (Å)	2.34	2.37
$\{[Hg(H_2O)_6]\,[H_2O]\}^{2+}$	E (au)	−575.8738	−576.1666
$[Hg(H_2O)_7]^{2+}$	E (au)	−575.8653	−576.1669
	R_{Hg-O1} (Å)	2.43	2.42
	R_{Hg-O2} (Å)	2.41	2.40
	R_{Hg-O3} (Å)	2.34	2.33
	R_{Hg-O4} (Å)	2.44	2.39
	$A_{O1-Hg-O2}$	141.3°	140.4°
	$A_{O1-Hg-O3}$	80.9°	80.3°
	$A_{O1-Hg-O4}$	76.3°	77.6°
$[Hg(H_2O)_8]^{2+}$	E (au)	−652.2161	−652.5119
	R_{Hg-O} (Å)	2.44	2.43
	A_{O-Hg-O}	118.1°	112.0°
H_2O	E (au)	−76.3256	−76.3382

[a] Energy values of the isolated water molecule and of the most stable isomer of the hexacoordinated cluster with one water molecule in the second shell are also reported.

(polarizable continuum model).[21,22] Full geometry optimizations lead to true energy minima (all positive Hessian eigenvalues) for hexa-, hepta-, and octacoordinated species with T_h, C_2, and S_8 symmetry, respectively (see Figure 3 and Table 5). Furthermore, displacement of one water molecule from the first solvation sphere of $[Hg(H_2O)_7]^{2+}$ leads, as already found for other metal ions,[37] to a structure retaining C_2 symmetry in which the seventh water molecule forms two hydrogen bonds with two water molecules of the first coordination sphere. The structure with one water molecule in the second shell is significantly more stable for the isolated clusters, but the hexa- and heptacoordinated species become nearly isoenergetic ($\Delta E = 0.0003$ au $= 0.8$ kJ/mol) when bulk solvent effects are taken into account through the PCM (see Table 5).

It is remarkable that such a strong solvent induced energy variation occurs with only negligible geometry modifications, i.e., a shortening by about 0.05 Å of a couple water molecules in the heptacoordinated species (Hg−O4 distance in Figure 3B and Table 5). Inclusion of nonpotential energy terms (zero-point energy, thermal enthalpic, and entropic contributions)[38] does not modify the results in an appreciable way. Thus, our QM computations suggest that in aqueous solution the Hg(II) ion could have a quite flexible coordination. Furthermore, charge transfer is negligible for all the studied systems (maximum charge of 0.02 on a single water molecule from a Mulliken population analysis), so that effective two-body potentials can be confidently derived.

In order to proceed further, we decided to perform a 60 ns long MD simulation of the Hg(II) ion in aqueous solution (at least 1 order of magnitude longer than the estimated residence time of water molecules in the first Hg(II) shell).[8] This simulation length allows one to predict the water exchange rate with the bulk of the liquid and to evidence transitions between different possible coordination geometries of the Hg(II) hydration complex. The long simulation time needed to evaluate water residence time and the ongoing discussion about the reliability of current density functionals in the description of water exchange mechanisms[37] do not allow the use of first principle extended Lagrangian dynamics. Thus, we resorted to fitting reliable two-body empirical Hg(II)−H_2O potentials from MP2 computations in a vacuum and to adding effective many-body contributions by the procedure validated in our previous studies, which relies on the proper use of PCM computations.[15,16]

As previously mentioned, the simulated system consists of one Hg(II) ion and 819 SPC/E water molecules,[28] and the simulation started from a hexacoordinated first shell configuration. After a quite long induction time (about 630 ps) the system goes to heptacoordination, which remains stable for most

(37) Rotzinger, F. P. *J. Phys. Chem. B* **2005**, *109*, 1510−1527.
(38) Barone, V. *J. Chem. Phys.* **2004**, *120*, 3059−3065.

of the remaining simulation time except for a few transitions to hexa- (Figure 3C) and octacoordinated clusters (8 and 13 transitions from hepta- to hexa- and octacoordinated clusters, respectively). It is noteworthy that during the induction time we observe a number of attempts of a seventh water molecule to enter the first solvation shell of Hg(II) resembling the results of previous short QM/MM simulations, which were interpreted in terms of a heptacoordinated transition state between two different hexacoordinated energy minima.[39] The obtained radial distribution function $g_{HgO}(r)$ (Figure 3D) shows a well-defined first solvation shell with a peak distance R_{HgO} of 2.28 Å and with a hydration number of 7 by integration up to 3.8 Å. The structural results, therefore, evidence the dominance during the simulation of the heptahydrated complex since the hexa- and octacoordinated species are present only for about 2.6 and 0.6% of the analyzed time (i.e., from 5 to 65 ns of simulation time), respectively. The longest lifetimes for the hexa-, hepta- and octacoordinated hydration shell are 0.37, 8.02 and 0.14 ns, respectively. The mean residence time of the water molecules in the first hydration shell is 7.4 ns, of the same order of magnitude of the experimental estimated value (about 1 ns), obtained by Eigen in 1963 with ultrasound absorption, where the rate constants are estimated from SO_4^{2-} complexation reactions.[8]

Inclusion of explicit many-body effects is crucial for the description of ions in aqueous solution,[40] and we have already shown for Cd(II) in water that the approach summarized by eq 2 accounts for averaged many-body terms in an effective two-body classical potential.[16] We have estimated the effect of many-body contributions in the Hg(II) hydrated system by comparing the results issuing from use of the complete effective potential with those delivered by a conventional pair additive potential, obtained by the in vacuum *ab initio* calculations of the Hg(II) ion and one water molecule at the MP2 level. The pure pair additive potential is more attractive and gives rise to a longer Hg−O coordination distance as compared to the effective two-body one, in the Hg(II)−water minimum configuration (Supporting Information Figure S2A). An additional MD simulation has been performed using the pure pair additive potentials (see forcefield parameters in Table 3), and the obtained radial distribution function $g_{HgO}(r)$ and hydration number $N(r)$ have been compared with the corresponding curves for the effective two-body potential (Supporting Information Figure S2B). The most evident effect of the use of a pure pair additive potential concerns the increase in the number of water molecules coordinated around the Hg(II) ion (9.5 by integration up to 3.8 Å), as compared to the hydration number obtained with the effective two-body potential (7 by the same integration). This finding closely parallels the reduction in coordination number (from 7.35 to 6 for the Mg(II) aqueous solution) found by Spångberg and Hermansson when adding three-body terms.[40,41] Moreover, in the case of the pure pair additive potential, the oxygen and hydrogen $g(r)$'s are not well separated between first and second hydration shells, indicating a more disordered coordination structure around the ion. Therefore, the inclusion of the many-body terms with our method has a clear effect on the structural and dynamic properties of the Hg(II) hydration shell, while its computational efficiency allows one to carry out extremely long MD simulations which are necessary to reproduce the dynamic properties of ionic solutions with flexible hydration shells.

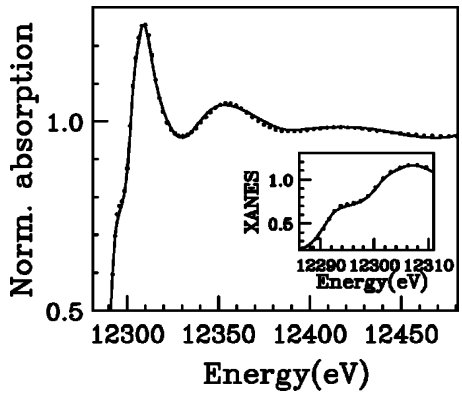

Figure 4. Comparison of the Hg L_{III} deconvolved experimental XANES spectrum of the Hg(II) aqueous solution (dotted line), with the best fit theoretical spectrum (solid line) as obtained from a heptacoordinated complex having a C_2 symmetry.

The combined QM and MD results strongly suggest that the hydrated Hg(II) ion is characterized by a quite flexible heptacoordinated structure whose energy minimum has a C_2 symmetry. Therefore, we reinterpreted the XANES spectrum in terms of a heptahydrated Hg(II) ion. We performed a minimization of the experimental data starting from the *ab initio* energy minimum structure of the $[Hg(H_2O)_7]^{2+}$ complex shown in Figure 3B, refining four structural parameters while retaining a C_2 symmetry (Figure 4). The Hg(II)−O distances obtained from the minimization procedure are reported in Table 4. The Hg(II)−O average distance is 2.31 Å in agreement with the EXAFS determination, and the R_{sq} value obtained was 1.6 (see Table 4).

A second fit was performed using an unconstrained heptacoordinated model where all seven Hg−O distances were refined separately. Also in this case a similar geometry was obtained from the minimization procedure with a Hg(II)−O average distance of 2.32 Å and $R_{sq} = 1.1$. The availability of new degrees of freedom in the minimization procedure does not significantly change the quality of the fit, and it produces a slightly different set of structural parameters, still corresponding to a C_2 symmetry. An additional fit of the experimental data was performed starting from a cluster having seven equal Hg−O distances arranged in a C_2 symmetry and keeping such a symmetry during the minimization by refining a single distance. The optimized Hg(II)−O distance is 2.30 Å, and the agreement between the experimental and theoretical data was not good ($R_{sq} = 15.0$), thus showing that the water molecules in the Hg−O heptacoordinated cluster are arranged in a less symmetrical fashion. Attempts to fit the XANES spectrum with a mixture of hexa- and heptahydrated clusters showed that the experimental data can be reproduced only for a strong dominance (higher than 90%) of the heptacoordinated species.

The picture emerging from these tests is both enlightening and intriguing. If a single first shell model cluster is used to fit the XANES data, the best agreement is obtained when a sevenfold coordination within a C_2 symmetry and a quite large distance dispersion (defined as the difference between the maximum and minimum Hg−O bond length) is considered (0.38

(39) Kritayakornupong, C.; Rode, B. M. *J. Chem. Phys.* **2003**, *118*, 5065−5070.
(40) Spångberg, D.; Hermansson, K. *J. Chem. Phys.* **2004**, *120*, 4829−4843.
(41) Curtiss, L. A.; Halley, J. W.; Hautman, J. *Chem. Phys.* **1989**, *133*, 89−94.

Å). However, the dispersion of distances obtained for the heptahydrated cluster from MP2 calculations is much smaller (0.09 Å, see Table 5), and this is also the case for the MD simulations (0.12 Å). Note that the distance dispersion along the MD simulation has been estimated selecting a window (Supporting Information Figure S3) around the longest lifetime of the heptacoordinated species. One might therefore conclude that a proper fit of the XANES data needs a wider distance dispersion than that obtained from the theoretical heptahydrate models. This discrepancy can be due to two main reasons: the need to account for the structural disorder within the first hydration shell in the analysis of the XANES data, and the influence of the second hydration shell on the low-energy range of the absorption spectrum.

Unfortunately, the effect of the high mobility of the second hydration shell does not allow construction of reliable static models including its effect. One must, therefore, resort to analysis of the XANES spectra by the microscopic description of the system derived from MD simulations, as done, for instance, with remarkable success for the case of Ni(II) and Cr(III) ions in aqueous solution.[42]

Ongoing application of the same procedure to a Hg(II) aqueous solution faces the need for major computer resources connected to the high atomic number of the photoabsorber atom and the flexibility of the hydrated structure. In the meantime, we thought it interesting to analyze a limited number of snapshots issuing from MD simulations, including all the water molecules providing nonnegligible contributions to the spectrum: this defines a cutoff radius of 5.2 Å from the cation and 17 water molecules. In particular, we have considered two sets of 10 snapshots each for the heptacoordinated complex (characterized by distance dispersions in the first shell of 0.12 and 0.28 Å, respectively) and a third set of 10 snapshots for the hexahydrated complex (with a distance dispersion of the ion in the first shell of 0.11 Å). The agreement between the experimental and theoretical spectra is much better for the heptacoordinated set with a small distance dispersion (average R_{sq} values = 5.2, 10.2, and 16.3, respectively). This suggests that the second hydration shell provides a detectable contribution to the XANES spectrum and that the wide distance dispersion obtained from the XANES minimization using a single representative configuration tries to mimic the contribution of the neglected second hydration shell. Moreover the compatibility of the XANES data with a heptahydrated Hg(II) first shell cluster is confirmed.

Conclusions

We have reported the main results of the first quantitative analysis of the XANES spectrum of a Hg(II) aqueous solution using the recently developed MXAN method, starting from QM ab initio and MD theoretical results. The combined use of XAS experimental data, accurate QM calculations, and MD simulations allowed us to determine, in contrast to all the previously reported results, a quite unexpected sevenfold coordination of the hydrated Hg(II) complex in aqueous solution. The generally accepted octahedral solvation structure of the Hg(II) ion could not be reconciled with XAS results, and refined QM computations pointed out the remarkable stability of a heptacoordinated structure with C_2 symmetry. Moreover, long-time MD simulations by new two-body interaction potentials, taking into account nonadditive solvent effects in an effective way, revealed that the hydrated complex undergoes frequent transformations among several flexible heptacoordinated complexes.

The best-fit model cluster, obtained from the XANES data analysis, shows a larger distance dispersion as compared to the MP2 and MD theoretical models. This discrepancy is most probably due to the necessity of including the second hydration shell in the calculation of the XANES spectra, and additional investigations are underway to shed light on this point.

In conclusion, while none of the separate techniques available to study metal ions in solution would be sufficient to give an unequivocal structural result, the coherent picture provided by accurate QM calculations, MD simulations, and XAS experimental results provides convincing evidence for a dynamical picture of the Hg(II) first hydration shell involving a flexible heptacoordinated cluster. This is at variance with the octahedral structure usually present in the solid state[43] and suggested by previous short time MD simulation.[39] These findings are exemplary in pointing out the limits of transferring solid-state results to assess the structural properties of metal ions in aqueous solutions, as already observed, for example, in the case of the Cu(II) hydrate in the solid state and solution.[44] The original application of both experimental and computational techniques used in the present research paves the route for the systematic use of an integrated approach, with increased reliability, in the structural investigation of liquid samples and biological media.

Acknowledgment. We gratefully acknowledge the CASPUR computational center for providing the computational resources used in this work.

Supporting Information Available: Figure S1, Hg L_3-edge X-ray absorption spectrum of Hg(II) aqueous solution before and after deconvolution. Figure S2, two-body and simple pair additive potentials of the Hg(II)−water minimum configuration and corresponding Hg−O radial distribution functions. Figure S3, distance dispersion of the Hg(II) heptahydrate cluster along the MD simulation. Complete ref 14. This material is available free of charge via the Internet at http://pubs.acs.org.

JA066943Z

(42) (a) D'Angelo, P.; Roscioni, O. M.; Chillemi, G.; Della Longa, S.; Benfatto, M. *J. Am. Chem. Soc.* **2006**, *128*, 1853−1858. (b) Merkling, P. J.; Muñoz-Páez, A.; Martínez, J. M.; Pappalardo, R. R.; Sánchez Marcos, E. *Phys. Rev. B* **2001**, *64*, 092201-4. (c) Merkling, P. J.; Muñoz-Páez, A.; Sánchez Marcos, E. *J. Am. Chem. Soc.* **2002**, *124*, 10911−10920. (d) Merkling, P. J.; Ayala, R.; Martínez, J. M.; Pappalardo, R. R.; Sánchez Marcos, E. *J. Chem. Phys.* **2003**, *119*, 6647−6654.

(43) Aekesson, R.; Persson, I.; Sandstrom, M.; Wahlgren, U. *Inorg. Chem.* **1994**, *33*, 3715−3723.

(44) (a) Benfatto, M.; D'Angelo, P.; Della Longa, S.; Pavel, N. V. *Phys. Rev. B* **2002**, *65*, 174205/1−174205/5. (b) Pasquarello, A.; Petri, I.; Salmon, P. S.; Parisel, O.; Car, R.; Toth, E.; Powell, D. H.; Fischer, H. E.; Helm, L.; Merbach, A. E. *Science* **2001**, *291*, 856−859. (c) Amira, S.; Spangberg, D.; Hermansson, K. *Phys. Chem. Chem. Phys.* **2005**, *7*, 2874−2880.